



Nitrous oxide and methane concentrations and air-sea fluxes in undersampled areas of the Mediterranean basin

5 Mercedes de la Paz¹, Susana Flecha², Fatima Zohra Bouthir³, Milad Fakhri⁴, Abed El Rahman Hassoun^{4,5}, Valeria Ibello⁶, Korhan Özkan⁶, Fiz F. Pérez¹, Adil Chair³, Iris E. Hendriks⁷

1 Instituto de Investigaciones Marinas (IIM-CSIC), Vigo, Spain

10 2 Instituto de Ciencias Marinas de Andalucía (ICMAN-CSIC), Puerto Real, Cádiz, Spain

3 Institut National de Recherche Halieutique (INRH), Casablanca, Morocco

4 National Centre for Marine Sciences, National Council for Scientific Research in Lebanon (CNRS-L), Beirut, Lebanon

5 GEOMAR Helmholtz Centre for Ocean Research Kiel, Kiel, Germany

15 6 Middle East Technical University, Institute of Marine Sciences, Mersin, Türkiye

7 Climate Change Research Group. Mediterranean Institute for Advanced Studies (IMEDEA-CSIC), Esporles, Spain

Correspondence to: mercedes.delapaz@iim.csic.es

Abstract: Nitrous oxide (N₂O) and methane (CH₄) are potent greenhouse gases for which oceanic contributions remain uncertain, particularly in undersampled regions like the Southwest and Southeast margins of the Mediterranean Sea, where there is a major observational gap. This data paper presents a comprehensive dataset of monthly N₂O and CH₄ concentrations and air-sea fluxes collected over a full seasonal cycle (April 2023 - June 2024 at most sites, with one station extended to September 2024) from eight coastal stations across three distinct Mediterranean ecoregions (Alboran, Balearic, and Levantine Seas) as part of the ROADSTER collaborative project. Sampling, preservation, and analytical procedures were standardized across sites, and dissolved-gas analyses were performed in a single laboratory to ensure comparability. We detail standardized sampling and analytical methodologies, including ancillary variables (temperature, salinity, dissolved oxygen, chlorophyll *a* and inorganic nutrients). The compiled dataset reveals distinct seasonal and spatial variability: N₂O concentrations exhibit a strong negative correlation with temperature, with all stations acting as moderate N₂O sources. Conversely, CH₄ concentrations show greater variability and a positive correlation with temperature, with the Levantine sub-basin stations displaying episodic high-flux events (up to 35.20 μmol m⁻² d⁻¹) indicative of localized seafloor sources. This dataset bridges significant data gaps in the Mediterranean, providing a crucial baseline for regional climate modeling, understanding biogeochemical processes, and future climate change impact assessments.

Keywords: Nitrous oxide, Methane, Greenhouse gases data, Mediterranean Sea, Coastal Ocean, Air-sea fluxes, Marine biogeochemistry



1. Introduction

40 Methane (CH₄) and nitrous oxide (N₂O) play critical roles in the atmospheric radiative balance and
the climate system (Ciais et al., 2013). Although their atmospheric budgets are largely controlled by
terrestrial sources and sinks, oceanic emissions represent an important component of their global
cycling, particularly in coastal regions where emissions of N₂O and CH₄ are being enhanced (Weber
et al., 2019; Saunois et al., 2020). The last synthesis of GHG fluxes in the global coastal ocean
45 developed by the Regional Carbon Cycle Assessment and Processes (RECCAP2), evidenced that
emissions of CH₄ and N₂O from the global coastal ocean can offset a substantial fraction of the
coastal uptake when expressed in CO equivalent radiative forcing, highlighting the need to consider
additionally N₂O and CH₄ gases when evaluating ocean–climate feedbacks (Resplandy et al., 2024).

The ocean thus acts as both a source and a sink of CH₄ and N₂O through a range of interacting
50 biogeochemical and microbial processes (Reeburgh, 2007; Codispoti, 2010). Global coastal and
oceanic CH₄ emissions are estimated at approximately 12 (6–20) Tg CH₄ yr⁻¹, arising from microbially
mediated production in marine sediments and the water column, as well as from geological
pathways, including hydrothermal vents, cold seeps, mud volcanoes and CH₄ clathrate seepages
(Reeburgh, 2007; Saunois et al., 2025). As a consequence, coastal ecosystems are increasingly
55 recognised as weak but spatially extensive net sources of CH₄ to the atmosphere (Weber et al.,
2019; Saunois et al., 2020). Similarly, N₂O accounts for about one-third of the natural sources to the
atmosphere (Ciais et al., 2013). This gas is microbially produced in the ocean mainly through
nitrification and denitrification, which are highly sensitive to dissolved oxygen levels and redox
conditions (Codispoti, 2010; Freing et al., 2012).

60 In this context, the Mediterranean Sea constitutes a particularly relevant system for investigating
marine CH₄ and N₂O dynamics. As a semi-enclosed basin with an extensive coastline and distinct
biogeochemical and hydrodynamic characteristics, it is recognised as a climate-change hotspot
(MedECC, 2020; Hassoun et al., 2025). Despite accounting for less than 1% of the global ocean
surface, the Mediterranean hosts a disproportionately high biodiversity and is highly vulnerable to
65 global warming, ocean deoxygenation, acidification, and increasing terrestrial nutrient and organic
matter inputs, especially in coastal zones (Bianchi and Morri, 2000; Mouillot et al., 2011; Hassoun et
al., 2025). These pressures are particularly pronounced in the western Mediterranean, subject to
intense coastal development and tourism, that has seen a dramatic increase in pollution and habitat
degradation, with only a small fraction of its coastline remaining in pristine condition (EEA, 1999).
70 Hence, all drivers of environmental change are expected to affect future biogeochemical cycles and
emissions of N₂O and CH₄ in the Mediterranean Sea.



75 Despite its ecological importance and vulnerability, the Mediterranean Sea remains understudied regarding non-CO₂ GHG emissions. Data availability of N₂O and CH₄ and is extremely scarce compared to other oceanographic regions, as evidenced by the RECCAP2 synthesis report of GHG in global coastal oceans, with only a few measurements available for the emission computations of N₂O and CH₄ (Resplandy et al., 2024). Also, previous studies assessing the N₂O and CH₄ patterns throughout the water column are limited to the western limit of the Mediterranean Basin, namely at the Gibraltar Strait, where the impact of vertical mixing at surface N₂O concentrations drives short-term temporal variability (de la Paz et al., 2015), and the Balearic Ocean Acidification Time Series (BOATS), where monthly observations show interannual and seasonal variability of N₂O and CH₄ since 2018 (Flecha et al., 2023; Flecha et al. 2025). Although studies on GHGs' vertical patterns in water columns in the Eastern Mediterranean are very limited (Bange et al 1996), there is multiple evidence of gas released from geological sources of CH₄ at the Eastern Mediterranean Seafloor, where there are gas seepages and mud volcanoes, pointing out the high gas hydrate potential of the Eastern Mediterranean Sea (Meroy and Longinos, 2019)

90 Expanding data collection in under-observed marine regions for non-CO₂ greenhouse gases, such as N₂O and CH₄, is vital given their significant contributions to global warming and ocean feedback mechanisms (Bange et al., 2019; Hassoun et al., 2024). In the Mediterranean Sea, data scarcity— together with the limited temporal and vertical resolution of existing observations—still hampers basin-wide extrapolations and a comprehensive understanding of ocean–atmosphere fluxes of these gases (Rosentreter et al., 2023; Resplandy et al., 2024). These observational gaps are further compounded by the lack of long-term, sustained resources for key databases such as MEMENTO, constraining our ability to assess variability and detect trends in N₂O and CH₄ distributions and fluxes (Rees et al., 2022).

100 To bridge these limitations, strengthening coordination among scientists working across the Mediterranean basin is essential for improving data coverage and advancing measurements and predictions of non-CO₂ GHG dynamics (Bange et al., 2019; Hassoun et al., 2022). Standardising measurement protocols and ensuring the availability of long-term, high-quality datasets are fundamental steps for reducing analytical biases and for improving our understanding of N₂O and CH₄ processes (Wilson et al., 2018; Bange et al., 2019). Establishing a more integrated ocean-observing network in the Mediterranean region will enhance the consistency of data collection and contribute to the development of a Findable, Accessible, Interoperable and Reusable (FAIR; 105 Tanhua et al., 2019) data baseline. Such harmonised and traceable observations are prerequisite for robust assessments of oceanic greenhouse-gas fluxes, for reducing uncertainties in emission estimates, and for supporting transparent reporting under international and regional policy frameworks, including the Paris Agreement and its Global Stocktake (UNFCCC, 2015; UNFCCC,



2023), as well as European environmental obligations such as the Marine Strategy Framework
110 Directive (European Commission, 2008).

As a product of the collaborative project between Eastern and Western Mediterranean countries
entitled “Greenhouse Gas dynamics on the southern coasts of the Mediterranean Sea”
(ROADSTER), this study provides a comprehensive dataset of monthly N₂O and CH₄ concentrations
115 and fluxes across vast, understudied areas of the Mediterranean Sea—the southwest and southeast
margins—over a full seasonal cycle. All gas measurements in seawater were performed in the same
laboratory, and sampling and storage protocols were standardised across participants to minimise
analytical bias (Wilson et al., 2018). This dataset offers the first combined assessment of seasonal
and temporal variability of N₂O and CH₄ across three Mediterranean ecoregions, providing a robust
120 baseline for understanding the processes driving temporal variability, informing future sampling
strategies, and supporting global biogeochemical modelling and upscaling efforts aimed at refining
estimates of oceanic CH₄ and N₂O emissions under ongoing climate and ocean-warming conditions.

2. Methods

125 The ROADSTER project, involving various research institutions from countries bordering the
Mediterranean Sea (namely Lebanon, Morocco, Türkiye, and Spain), aimed to conduct a year-long
series of monthly surface water measurements of N₂O and CH₄ at established coastal oceanographic
stations. Sampling was conducted monthly at eight oceanographic stations across the
Mediterranean, which were categorised into three marine regions: the Levantine Sea (Lebanon:
130 LEV-B1, LEV-BEY2, and Türkiye: LEV-ETS), Balearic Sea (Spain: BAL-CA, BAL-CS, and BAL-PB),
and Alboran Sea (Morocco: ALB-M'DIQ and ALB-REM).

Measurements encompassed dissolved N₂O and CH₄, along with ancillary variables pertinent to the
biogeochemical cycles of N₂O and CH₄, such as temperature (T), salinity (S), dissolved oxygen (O₂),
135 chlorophyll *a* (Chl*a*), and inorganic nutrients (nitrite, nitrate, phosphate and silicate). At the start of
the project, detailed standardised protocols for the collection, preservation, and storage of gas
samples until analysis were disseminated to participating laboratories. Additionally, the standardised
equipment for gas sampling were distributed to ensure methodological consistency across
participating laboratories and sampling initiatives.

140

2.1 Site description and sampling strategy

2.1.1 Morocco

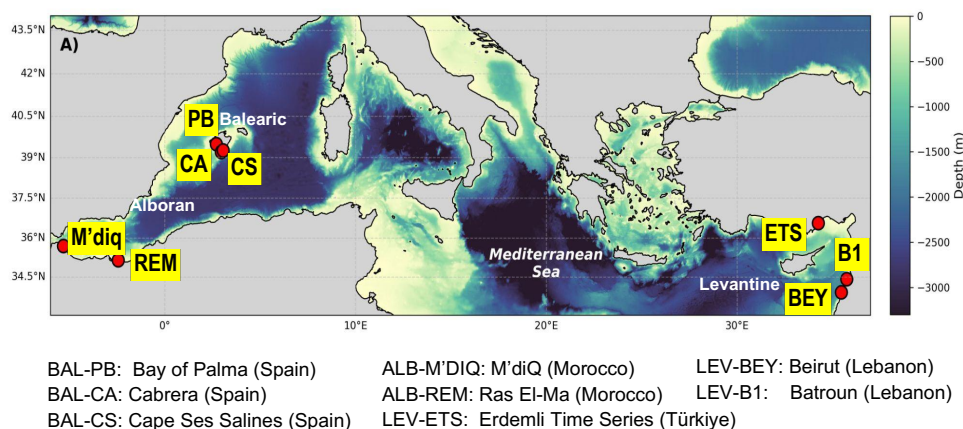
145 The Mediterranean coast of Morocco was surveyed for 13 months from April 2023 to May 2024 at
two sites, which are conditioned by the public health protection vocation of the INRH (National



Institute for Fisheries Research) network, i.e. in the vicinity of shellfish production areas in the coastal domain. The stations, namely ALB-M'DIQ and ALB-REM, are located in the region of the Alboran Sea, characterised by the entrance of surface North Atlantic Water in the upper layer entering to the Mediterranean coinciding with the outflow of Mediterranean Water at the deeper layer, and the consistent presence of eddies and coastal upwelling that are modulated by mesoscale wind regime and complex hydrodynamics in the nearby Strait of Gibraltar (Macias et al, 2006).

150

160



165

Figure 1. Map of the Mediterranean Sea showing the locations of sampling sites (red dots) and the acronyms used in the text.

The ALB-M'DIQ station is characterized by a typically Mediterranean climate, influenced by offshore Mediterranean water masses and by episodic deep-water upwelling, with an annual mean temperature of 12.5°C and an annual total precipitation of 143 mm in 2023 (<https://fr.tutiempo.net/climat/ws-603400.html>). The site is located 800 m from the coast, with 10 m bottom depth, and was characterized by the highest content of sandy-silt, with no vegetation. The site is near the fishing harbor and marina in the town of M'diq, with a population of c. 100.000, and is subject to various anthropic pressures such as aquaculture activities and to effluent discharges, especially in summer.

175

The ALB-REM station is located in the north-east of Morocco, with a typically Mediterranean and dry climate, an annual mean temperature of 19.9°C and an annual total precipitation of 374 mm in 2023 (<https://fr.tutiempo.net/climat/ws-603400.html>). The site is located 1 km from the coast, over 30 m bottom depth and on a continental shelf with a gentle slope, consisting of sandy bottom without any vegetation, and 10 km west of the estuary of the Moulouya river (600 km long and the second largest in the North African coast only behind the Nile Delta). The site is near the fishing harbor of the Ras El-Ma village with a population of c. 20.000. Both sites are close to ports and fish farms.

180



185 Samples for N_2O and CH_4 , Chl a , and inorganic nutrients were collected onboard an INRH small vessel. Water samples were collected using Niskin bottles at a depth of approximately 1 m. Hydrological parameters were measured using a Pro DSS Multiparametric sensor (Table 1).

2.1.2 Spain

190 Physicochemical and biogeochemical data were collected from three stations in the Balearic Sea, part of the Balearic Ocean Acidification Time Series (Flecha et al., 2022). The first station, located in the Bay of Palma (BAL-PB: ~30 m bottom depth), is part of the Balearic Islands Coastal Observing and Forecasting System monitoring network (SOCIB; <https://www.socib.es/>). Hourly measurements of temperature, salinity and O_2 were recorded with autonomous sensors. The second station is located in the Bay of Santa Maria, Cabrera Archipelago National Park (BAL-CA: ~8 m depth), a
195 pristine area under governmental protection. Similar parameters (temperature, salinity, pH and O_2) were measured with high-precision sensors. Both BAL-PB and BAL-CA are fixed monitoring stations, with data collected monthly from depths of 1 and 4 m, respectively. The third site is in the coastal area near the Cape Ses Salines lighthouse (BAL-CS: ~2 m bottom depth), where surface water samples were collected biweekly, starting in August 2022 for O_2 measurements. Samples for
200 dissolved CH_4 and N_2O concentrations and inorganic nutrients were also collected at all sites. Inorganic nutrient samples were analyzed using the Autoanalyser AA3 HR (Seal Analytical) via continuous-flow analysis. The precision, estimated from the coefficient of variation based on replicate analyses of the same water samples ($n = 10$), ranged from 0.13 % to 0.5 %.

205 The BOATS network surface layer is characterized by Modified Atlantic Water (MAW). There is no continuous freshwater contribution or significant anthropogenic pressures in BAL-CA or BAL-CS. Although BAL-PB could be affected by anthropogenic activities due to its proximity to urban areas, previous data analysis in this time series show no significant differences among stations for N_2O and CH_4 (Flecha et al., 2023; Flecha et al., 2025). Water samples were collected at BAL-PB and BAL-CA using a water pump and at BAL-CS directly from the coast (Table 1).

210

2.1.3 Lebanon

215 Samples in Lebanon were collected from two coastal stations: 1) LEV-B1 is located offshore Batroun city, Northern Lebanon (Table 1, Fig. 1) and is an inshore time-series station close to Batroun's port with a maximum depth of ~8 m, 2) LEV-BEY is a coastal station located offshore of Beirut, the Lebanese capital, and is surrounded by many infrastructure facilities (mainly recreational ones). Monthly monitoring of key physic-chemical parameters has been conducted since 1991 at station LEV-B1 (Hassoun et al., 2021) and for 30 years ago at station LEV-BEY. Both stations are sampled on a monthly basis and include measurements of a broad range of physical, chemical, and biological parameters. In addition, analysis of temperature records since 1999 indicates a significant warming
220 trend of approximately 0.09 °C per year (Ouba et al., 2016).



The thermohaline properties were similar to those of the Levantine Sea Water source type. Sampling was conducted monthly between May 2023 and June 2024 to collect surface water samples. *In situ* temperature measurements were conducted using a standard surface thermometer. Salinity was
225 determined using a Beckman salinometer, model R S7-C, with a precision of $\pm 0.01^\circ\text{C}$ for temperature and ± 0.1 for salinity. For O_2 analysis, samples were first extracted from the Niskin bottle and concentrations were determined using Winkler titration (Hansen, 1999), with a precision of ± 15 $\mu\text{mol kg}^{-1}$. Phosphate concentrations were measured according to the method described by Murphy and Riley (1962) using a ThermoSpectronic Helios spectrophotometer, with a precision of ± 0.015
230 $\mu\text{mol kg}^{-1}$. Nitrites ($N\text{-NO}_2$) based on the method described by Bendshneider and Robinson (1952) and Nitrates ($N\text{-NO}_3$) following the method of Strickland and Parsons (1968), with a small modification from Grasshoff, (1961). Samples for total Chl *a* were filtered (Whatman GF/C) at a low pressure, and pigments were then extracted in 90% acetone and determined by a spectrophotometer according to Lorenzen (1967).

235
In LEV-B1 and LEV-BEY, observed biogeochemical variability is strongly influenced by seasonal and interannual changes in phytoplankton biomass, organic matter cycling, and episodic nutrient inputs. Previous studies in Lebanese coastal waters show recurrent spring and autumn chlorophyll-*a* maxima, reflecting enhanced primary production driven by winter mixing, transitional stratification,
240 and episodic nutrient supply (Abboud-Abi Saab et al., 2012; Ouba et al., 2016). In addition, land-derived nutrient and organic matter inputs, including river discharge, coastal runoff, and wastewater effluents, have been identified as important local drivers modulating productivity and biogeochemical signals along the Lebanese margin (Abboud-Abi Saab et al., 2012; Hassoun et al., 2019).

245 **2.1.4 Türkiye**

Seawater samples were collected at the most Eastern Mediterranean coast of Türkiye (LEV-ETS), a highly oligotrophic area, dominated by the Asian Minor Current flowing from east to west in the offshore waters (Fach et al. 2021). The LEV-ETS station is situated 600 meters from the coastline, at a depth of 25 m, on a continental shelf characterized by a gentle slope and a sandy bottom devoid
250 of vegetation. It is located near the town of Erdemli, which has a population of approximately 150,000. The area is subject to coastal eutrophication due to urban and agricultural pressures from the surrounding catchment area. The site is located 800 m east of Lamas River with an annual average discharge of $2.3 \text{ m}^3 \text{ s}^{-1}$ between 2010-2015 (General Directorate of State Water Affairs). The site has a hot, dry Mediterranean climate with an annual mean temperature of 19°C and an
255 annual total precipitation of 569 mm (Turkish State Meteorological Service, 2024, <https://mgm.gov.tr/>, accessed August 1, 2024). The site has been monitored monthly between June 2023 to September 2024 by METU Institute of Marine Sciences. Based on a ten-year average of



260 physico-chemical measurements ($n = 2735$), the site is characterized by a 22.65 ± 4.7 °C water temperature, 39.02 ± 0.63 salinity, $\pm 225.6 \pm 24.3$ $\mu\text{mol kg}^{-1}$ for O_2 , 0.86 ± 0.96 μM for Dissolved Inorganic Nitrogen (DIN) and 0.38 ± 0.35 $\mu\text{g L}^{-1}$ for Chl *a*. The samplings cruises were conducted onboard RV-Lamas and water samples were collected using Niskin bottles at c. 1-2 m depth. CTD casts were made using Seabird or YSI Exo2 sensors. Due to logistical issues with the CTD, there are certain months ($n=5$) with missing salinity and temperature. The N_2O and CH_4 gas samples from these specific cruises were still taken into consideration in our study while temperature and salinity
 265 were filled with data from the Mediterranean Sea Physical Reanalysis Product (MEDSEA_MULTIYEAR_PHY_006_004; Escudier et al., 2020) and compared with the climatological time series of temperature and salinity, with good agreement.

270 **Table 1.** Country, station code and nearest city and code of the sampling sites, geographic coordinates, sampling period for N_2O and CH_4 , number of cruises, ancillary variables.

Country Oceanographic region	Site Station Code	Location	Bottom Depth (m)	Gases Sampling period	Sampling cruises (n)	Ancillary Variables	Research Institution cruises
Spain Balearic Sea	Cabrera BAL-CA	39.15 °N 2.95 °E	8	05/2023 06/2024	13	T, S, Nuts, O_2 , Chl <i>a</i>	IMEDEA-CSIC
	Cape Salines BAL-CS	39.27 °N 3.05 °E	2	05/2023 06/2024	13	T, S, Nuts, O_2 , Chl <i>a</i>	IMEDEA-CSIC
	Palma Bay BAL-PB	39.49 °N 2.70 °E	30	05/2023 06/2024	13	T, S, Nuts, O_2 , Chl <i>a</i>	IMEDEA-CSIC
Lebanon Levantine Sea	Batroun LEV-B1	34.42 °N 35.75 °E	8	05/2023 06/2024	12	T, S, Nuts, O_2 , Chl <i>a</i>	CNRS-L
	Beirut LEV-BEY	33.90 °N 35.47 °E	3	05/2023 06/2024	14	T, S, Nuts, Chl <i>a</i>	CNRS-L
Türkiye Levantine Sea	Erdemli Time Series LEV-ETS	36.56 °N 34.25 °E	25	06/2023 09/2024	12	T, S	METU-IMS
Morocco Alboran Sea	M'diq ALB- M'diq	35.69 °N -5.32 °E	10	04/2023 04/2024	13	T, S, Nuts, O_2 , Chl <i>a</i>	INRH
	Ras El Ma ALB-REM	35.15 °N -2.45 °E	30	04/2023 04/2024	13	T, S, Nuts, O_2 , Chl <i>a</i>	INRH



275 2.2 Dissolved N₂O and CH₄ measurements

To ensure consistency across all sites, identical sampling materials and detailed protocols for N₂O and CH₄ were prepared and distributed to each collaborating laboratory. Before the start of the sampling cruises, dedicated training sessions on trace gas sampling were provided to all teams, aiming to harmonize procedures and minimize potential biases between sites and laboratories.

280 Duplicate samples for N₂O and CH₄ were collected in 120 mL borosilicate serum vials, sealed with grey chlorobutyl septa and aluminium crimps. To preserve the samples, approximately 200 µL of saturated HgCl₂ solution was added and the vials were stored upside down in the dark until analysis at the AQUANITROMET laboratory (de la Paz and Pérez, 2026) of the Instituto de Investigaciones Marinas (IIM-CSIC, Vigo, Spain).

285 The dissolved concentrations of N₂O and CH₄ were analysed using the static-headspace equilibration technique combined with gas chromatography following de la Paz et al., (2015, 2021). It consists of creating a headspace by automatically introducing a volume (20 mL) of ultrapure N₂ gas into the sample vial using a high-precision automatic burette displacing the same volume out of the vial by piercing the septum with two needles. After reaching equilibrium overnight in a
290 temperature-controlled environment, 18 mL of the headspace is automatically extracted using a high-precision burette and injected into a gas chromatograph (Agilent GC 7890-A), where the signal for each gas is separated using two independent Porapak Q-packed columns. Finally, N₂O is detected with an electron capture detector and CH₄ with a flame ionization detector. For the calibration curve, we used triplicate injections of three combined gas standard mixtures of N₂O and CH₄ in N₂, supplied
295 by NOAA (N₂O:CH₄=332:1959 ppb) and by AirLiquide France (ratios N₂O: CH₄=1000:3000 and 3100:5000 ppb). The precision estimated from the averaged coefficient of variation of duplicates (n=123) for this study was 1% for N₂O and 4.5% for CH₄. Detection limits (LOD) of N₂O and CH₄ have been estimated based on the standard error (E) and slope (b) of the calibration regression fitting (LOD = 3.3 E/b). The minimum detectable level of N₂O in the equilibrated headspace is 5
300 ppb, and 1.5 ppb for CH₄. This analytical system was intercalibrated with other laboratories, with very good results, as part of activities during the first large international experiment to compare marine N₂O and CH₄ measurements, organized by the Scientific Committee on Oceanographic Research (Wilson et al., 2018).

305 The gas concentration using the headspace equilibration was computed following Wilson et al. (2018):

$$C_{meas} [\text{nmol L}^{-1}] = \left(\beta x P V_{wp} + \frac{xP}{RT} V_{hs} \right) / V_{wp}$$

where β denotes the Bunsen solubility coefficient of N₂O (Weiss and Price, 1980) and CH₄
310 (Wiesenburg and Guinasso, 1979) expressed in nmol L⁻¹ atm⁻¹; x is the dry gas mole fraction (ppb) determined in the headspace; P is the ambient atmospheric pressure (atm); V_{wp} and V_{hs} are the



volumes of the water sample and equilibrated headspace, respectively (mL); R is the universal gas constant ($0.08205746 \text{ L atm K}^{-1} \text{ mol}^{-1}$); and T is the equilibration temperature (K). The CH_4 and N_2O concentrations are also expressed as percent saturation (N_2OSat and CH_4Sat in %), calculated as
315 the ratio between the measured concentration (C_{meas}) and the equilibrium concentration in seawater (C_{equi}) for each gas. The equilibrium concentrations were computed by multiplying Bunsen solubility coefficient (β) of each gas by the monthly average atmospheric molar fraction of N_2O and CH_4 measured at the Lampedusa monitoring station—the only site in the Mediterranean Sea with continuous records of these gases—obtained from the NOAA (National Oceanic and Atmospheric
320 Administration, USA) monitoring network (Lan et al., 2025).

Due to the lack of proper QC tools or reference materials for N_2O and CH_4 , such as those available for the carbonate system (CRMs produced by A. Dickson at Scripps USA), our QC procedure relied on replicate seawater samples and reported results as the coefficient of variation (CV, %). The
325 presence of outliers was established based on the CV value; hence, samples were discarded with a CV higher than 4.5% ($n=3$) for CH_4 and 1% for N_2O ($n=1$). In addition, some glass flasks were broken during transport to Vigo ($n=14$), reducing the total number of duplicate samples.

2.3 Calculation of N_2O and CH_4 air-sea fluxes

330 The air-sea fluxes (F) were calculated using the following formula:

$$F = k_w (C_{\text{meas}} - C_{\text{equi}})$$

where k is the gas transfer velocity (cm h^{-1}) and ($C_{\text{meas}} - C_{\text{equi}}$) is the air-sea concentration gradient of N_2O and CH_4 . By convention, and following the sign of the gas concentration gradient, negative
335 values of F correspond to a transfer of N_2O or CH_4 from the atmosphere to the ocean (i.e., a sink for the atmosphere) and positive values of F correspond to a transfer of those gases from the ocean to the atmosphere (i.e., a source for the atmosphere). There is a long-term debate over which is the best expression for gas transfer rate k, but here we adopted as the expression given by Wanninkhof et al. (2014), since it is widely used in the last RECCAP2 analysis for GHG emissions in the coastal
340 ocean (Resplandy et al., 2024). The gas transfer velocity by Wanninkhof (2014), gave the expression $k_w = 0.251 \langle U^2 \rangle (Sc/660)^{-0.5}$, where $\langle U^2 \rangle$ is the average of the square wind speed and Sc is the Schmidt number (dimensionless). For our study, due to lack of local sources for wind data on land or buoy for some of the stations, we used the monthly averaged of the square of 6 hourly wind data provided by the Cross-Calibrated Multi-Platform Ocean Surface Wind Vector 3.0 (CCMP) wind data
345 product that combines satellite and buoy data with model predictions (Wentz et al., 2015). This wind speed product is the optimum choice using the k proposed by Wanninkhof (2014), which is computed using this same data product, and has been demonstrated to be an optimum wind source for coastal regions (Otero et al., 2013). The Sc, dependent on the temperature, salinity, and specific gas



molecule, is calculated according to the coefficients for N_2O and CH_4 and the equation reported by
350 Wanninkhof (2014). Then, the Schmidt number for the *in situ* salinity at the Mediterranean station
was calculated by interpolating Sc for fresh water and seawater.

To determine the annual average air-sea fluxes of N_2O and CH_4 at each station, calculations were
performed over a 12-month period. Missing monthly values of N_2O , CH_4 , temperature, and salinity
during this timeframe were reconstructed through temporal linear interpolation based on the closest
355 available cruise measurements.

2.4 Analysis of the variability of spatial and temporal variability of N_2O and CH_4

To determine whether the differences in N_2O and CH_4 concentrations and other variables across
360 stations were statistically significant, we used Tukey's test with a significance level of $p < 0.05$.
Additionally, we compute the Spearman correlation coefficients between surface water CH_4 and
 N_2O concentrations and potential environmental factors, such as water temperature, salinity,
dissolved oxygen, inorganic nutrients, and Chl *a*. All analyses were done using the R software.

365 3. Results

Besides specific N_2O and CH_4 measurements, we detail the environmental setting and primary
oceanographic processes influencing the variability of measurements conducted in our study, while
also providing initial insights for future in-depth biogeochemical studies in the region.

A total of 111 observations of N_2O and CH_4 were obtained between April 2023 and June 2024 (except
370 for LEV-ETS, where observations were extended to September 2024), accompanied by
measurements of temperature, salinity, dissolved oxygen, Chl *a*, and nutrients (NO_3 , NO_2 , PO_4 , and
 SiO_2). Temporal coverage is uniform across stations, with one sampling event per month, except for
minor gaps due to logistical problems with ship availability or inclement weather.

3.1. Seasonal variability of N_2O and CH_4 concentrations

375 Overall, the seasonal variability of sea surface temperature (SST) was very similar in every region,
ranging from 14.5 °C in BAL-PB (March 2024) to 31.2 °C in LEV-BEY (August 2023) (Fig. 2). ALB-
M'DIQ exhibits unique characteristics, particularly the unexpectedly low temperatures observed
during the summer. These anomalies are likely linked to the eddy-driven vertical motion in the
Alboran sub-basin. This connection is supported by several studies that have documented
380 mesoscale eddies with intensified vertical motion and subsurface anticyclonic eddies along the
African coast (Tintoré et al., 1991; Viudez et al., 1998). Hence, except for ALB-M'diq, the maximum
(August) and minimum surface temperatures (from December to March) showed an overall



synchronised cycle between the stations, with lower seasonal SST amplitudes in the southern coast
of the Alboran sub-basin (9.5 °C ALB-REM) to higher seasonal SST amplitudes in the stations of the
385 Balearic Sea (13.3 °C in BAL-PB).

The sea surface salinity ranged from 36.6 in BAL-CS in June 2024 to 39.5 in LEV-ETS (Fig. 2b).
Compared to the other regions, the seasonal cycle of salinity was clearly observed in the surface
waters of Lebanon, where both stations LEV-B1 and LEV-BEY showed higher salinity values from
390 July to November, owing to intense evaporation and lower values from January to April owing to
precipitation/continental runoff (Abboud-Abi Saab et al., 2012).

Seasonal variability in N₂O concentrations was observed at all stations, with concentrations
increasing during winter and reaching minimum values in summer (Fig. 2, Table 2). The highest
395 N₂O concentration of 9.95 nmol kg⁻¹ was measured in BAL-PB in January 2024, whereas the
minimum N₂O concentration of 6.3 nmol kg⁻¹ corresponded to LEB-B1 in August of 2023. Monthly
N₂O concentrations showed a clear intra-annual cycle, with amplitudes ranging from 1.3 nmol kg⁻¹ in
ALB-M'DIQ to 3.1 nmol kg⁻¹ in BAL-PB Bay, which were directly correlated with SST amplitude.
Despite some inter-station differences, the timing of the peaks and troughs was broadly consistent
400 across the Mediterranean coast.

The CH₄ concentrations in surface waters ranged from 2.9 nmol kg⁻¹ measured in March 2024 in
BAL-CA to 38.2 nmol kg⁻¹ measured in September 2023 in LEV-ETS (Table 2). The distribution of
CH₄ concentrations were very skewed, and the minimum CH₄ was comparable between the stations
405 (60% of values were lower than 5 nmol kg⁻¹), and CH₄ peaks were evenly distributed and consistently
high along the coast of the Levantine sub-basin. Only BAL-CS showed a moderate seasonal trend,
with a gradual increase in CH₄ concentrations in June, peaking in July, and gradually decreasing
through September 2023. Apart from this, no clear seasonal pattern was observed for CH₄
concentrations.

410 The saturation status of N₂O in surface water for most of the period was oversaturated (Fig. 2, Table
2), except in May 2023 at the stations of the Balearic sub-basin (BAL-CS, BAL-CA) and in ALB-
M'DIQ in October 2023 and May 2024 with a moderate seasonal trend of lower N₂OSat in winter and
spring, and higher oversaturation in summer months, with the N₂OSat ranging from 96 ± 0% in BAL-
415 CS in May 2023 and 127 ± 1% in LEV-ETS in September 2023. The surface water at all the stations
was supersaturated in CH₄ (Fig. 2, Table 2), with minimum values during the winter and early spring
(110±4% in BAL-CA in March 2024) and higher values in summer (up to 400%), with very high
CH₄Sat peaks in the eastern Basin of the Levantine sub-basin that reached the 1973 ±4%



Table 2. Summary of the results using the entire database. The table shows the average, minimum (min), median, and maximum (max) values for temperature (°C), salinity, dissolved CH₄ concentration (mmol kg⁻¹), CH₄ saturation percent (CH₄ Sat %), dissolved N₂O concentration (mmol kg⁻¹), N₂O saturation percent (N₂O Sat %) in the surface water for every station

Station	Mean ±SD	Salinity	Temperature (°C)	CH ₄ (mmol kg ⁻¹)	SatCH ₄ (%)	N ₂ O (mmol kg ⁻¹)	SatN ₂ O (%)	Dissolved Oxygen (µmol kg ⁻¹)	Chl a (mg L ⁻¹)	Nitrate (µM)	Nitrite (µM)	Fostate (µM)	Silicate (µM)
BAL-CA	Mean	37.40	20.4	3.8	165	8.1	105	228	0.06	0.18 ±	0.03	0.32	0.6
	±SD	±0.24	±4.7	±0.8	±48	±1.0	±4	±20	±0.07	0.12	±0.04	±0.53	±0.2
BAL-CA	min	37.10	14.8	2.9	110	6.7	98	195.21	0.00	0.06	0.00	0.00	0.05
	max	38.00	27.5	5.6	277	9.3	110	254.93	0.16	0.38	0.14	1.91	0.89
BAL-CS	Mean	37.42	21.5	4.7	211	7.8	104	235	0.08 ±	1.97 ±	0.05 ±	0.12 ±	0.3
	±SD	±0.42	±4.4	1.4 ±	±80	±0.9	±3	±18	0.06	1.62	0.06	0.16	±0.2
BAL-CS	min	36.60	15.1	2.9	113	6.6	9	209.39	0.00	0.23	0.00	0.01	0.07
	max	37.90	28.1	8.0	399	9.2	110	259.54	0.17	6.27	0.22	0.70	0.77
BAL-PB	Mean	37.44	21.1	4.1	180	8.3	108	232 ± 17	0.08 ±	0.36 ±	0.06 ±	0.18 ±	2.1
	±SD	±0.21	±5.0	±0.8	±44	±1.1	±4	±16	0.09	0.47	0.05	0.23	1.1 ± 1.6
BAL-PB	min	37.10	14.5	3.0	129	6.8	101	208.88	0.00	0.03	0.01	0.00	0.41
	max	37.80	27.8	5.5	275	10.0	117	254.82	0.30	1.26	0.14	0.80	6.14
LEV-B1	Mean	38.80	24.5	6.9	323	7.3	111	212	0.19	1.21	0.06	0.99	2.1
	±SD	±0.39	±3.8	±1.7	±80	±0.6	±5	±16	±0.12	0.6 ± 0.62	±0.04	±2	±1.2
LEV-B1	min	38.02	18.9	4.7	223	6.3	102	183.49	0.05	0.14	0.02	0.01	0.80
	max	39.24	30.4	10.5	516	8.2	118	241.98	0.53	2.84	0.15	6.23	5.61
LEV-BEY	Mean	38.82	25.3	8.1	383	7.4	116	--	0.45	1.21	0.1	0.07	2.2
	±SD	±0.36	±3.7	±5.2	±243	±0.5	±11	--	±0.22	±2.03	±0.07	±0.04	±1.6
LEV-BEY	min	38.32	20.1	4.4	192	6.4	106	--	0.14	0.12	0.02	0.01	0.91
	max	39.26	31.2	18.2	900	8.0	145	--	0.84	7.78	0.25	0.15	6.93
LEV-ETS	Mean	39.23	24.2	13.6	659	7.2	112	--	--	--	--	--	--
	±SD	±0.46	±4.6 ±	±9.8	±499	±0.7	±7	--	--	--	--	--	--
LEV-ETS	min	38.63	18.8	4.7	237	6.3	104	--	--	--	--	--	--
	max	39.56	29.8	38.2	1973	8.2	127	--	--	--	--	--	--
ALB-MIDIQ	Mean	37.18	17.7	4.9	199	8.5	104	245	0.27	0.44	0.09	0.07	0.3
	±SD	±0.33	±1.8	±1.5	±58	±0.3	±4	±9	±0.23	±0.25	±0.1	±0.05	±0.2
ALB-MIDIQ	min	36.75	15.6	3.6	142	7.7	97	231.45	0.00	0.05	0.01	0.03	0.03
	max	37.81	22.2	9.3	366	9.1	111	255.10	0.89	0.78	0.38	0.21	0.68
ALB-REM	Mean	37.18	20.3	4.5	194	8.1	107	225	0.08	0.61	0.25	0.1	0.4
	±SD	±0.12	±3.2	±0.8	±37	±0.5	±4	±12	±0.07	±0.43	±0.28	±0.06	±0.2
ALB-REM	min	37.01	16.8	3.9	157	6.9	102	202.49	0.02	0.09	-0.08	0.05	0.09
	max	37.40	26.3	6.1	259	8.6	114	243.68	0.29	1.35	0.68	0.22	0.74

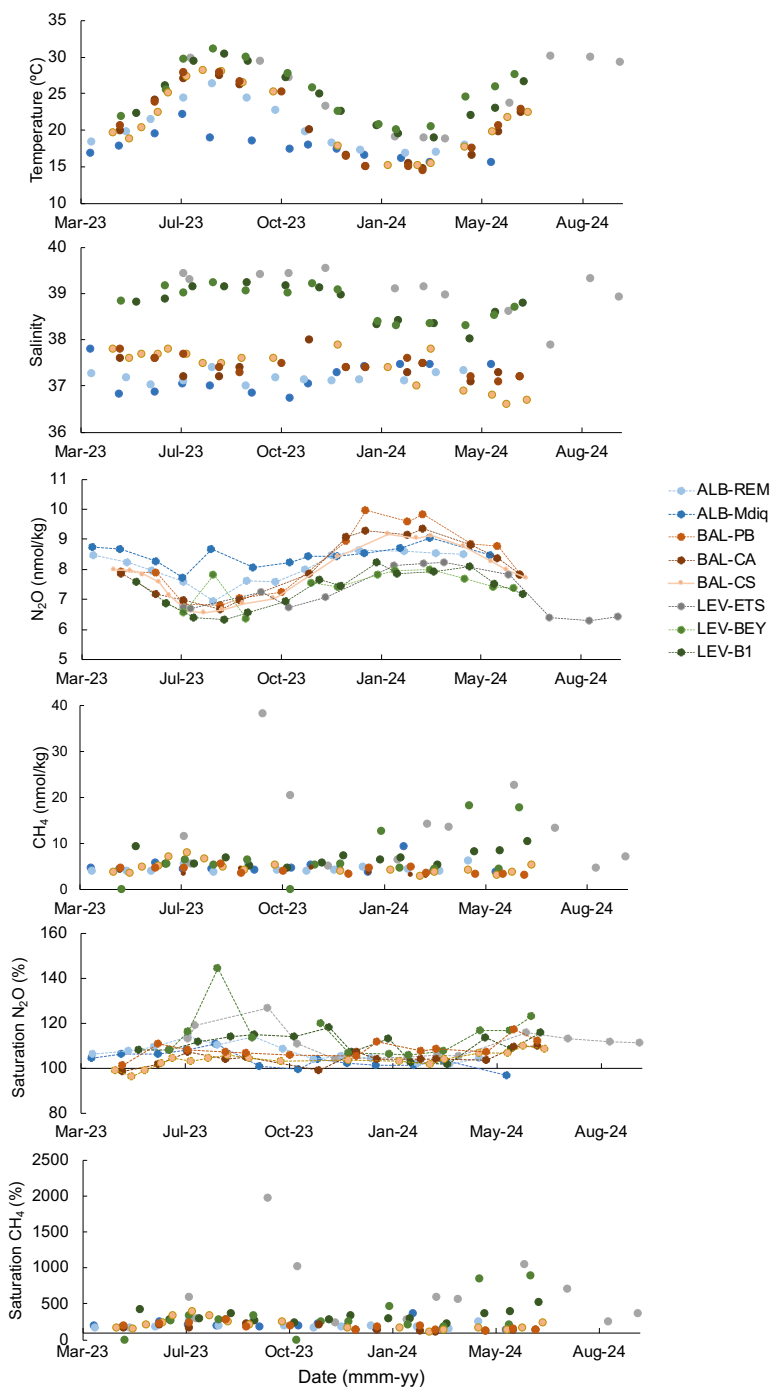


Figure 2. Time series data from the study sites, from top to bottom for temperature, salinity, dissolved N₂O and CH₄ concentration and saturation percent (expressed as nmol kg⁻¹ and % saturation) over the sample period.



425 **3.2. Spatial variability and annual mean regional distribution of N₂O and CH₄ on coastal waters
on the Mediterranean Basin scale.**

Sea Surface Temperature distribution was relatively homogeneous within each subbasin (Fig. 3) (Tukey test; $p > 0.05$). However, a significant longitudinal gradient was observed across the
430 Mediterranean Sea. The mean SST increased from 17.7 ± 1.8 °C at the westernmost station (ALB-M'diq, Alboran Sea) to 25.6 ± 4.6 °C at the easternmost station (LEV-ETS, Levantine Sea). Consequently, SST values were significantly higher in the Levantine Sea (B1, BEY, and ETS) compared to those in the Alboran and Balearic sub-basins (M'Diq, REM, and CA; $p < 0.05$), while no significant differences were found between the latter two subbasins. A similar zonal trend was found
435 for salinity, with mean values increasing from 37.18 ± 0.12 in Alboran coastal waters to 39.11 ± 0.46 in the Levantine sub-basin. This reflects a significant salinification in the Eastern basin (ETS, B1, and BEY) compared to the western Moroccan coast (M'diq, REM) and the Balearic sub-basin (CS, CA, PB), with a maximum inter-basin gradient of 1.9.

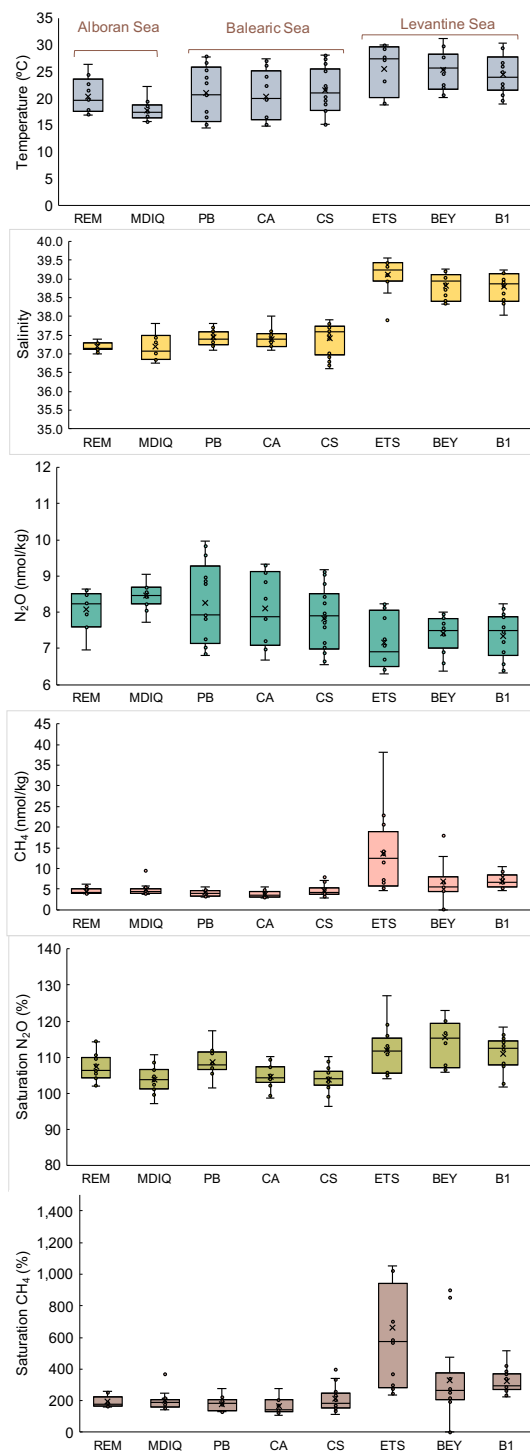
The regional distribution of CH₄ across the Mediterranean Sea exhibited a marked longitudinal
440 contrast (Fig. 3). Although temporal variability was systematically higher in the eastern stations, significantly elevated mean CH₄ concentrations were only observed at LEV-ETS (13.6 ± 9.8 nmol kg⁻¹; Tukey's test, $p < 0.05$). In the remaining stations, average concentrations ranged from 3.8 ± 0.8 nmol kg⁻¹ at BAL-CA to 8.1 ± 5.2 nmol kg⁻¹ at LEV-BEY. Despite the occurrence of high episodic values at LEV-B1 and LEV-BEY, their median concentrations did not differ significantly from those
445 in the Alboran and Balearic sub-basins (Tukey's test, $p > 0.05$). Surface waters throughout the Mediterranean Sea were persistently supersaturated in CH₄, with mean saturation levels ranging from $168 \pm 46\%$ (BAL-CA) to $659 \pm 500\%$ (LEV-ETS), following the spatial pattern of absolute concentrations. The CH₄Sat oversaturation peaks along with their associated variability observed at the LEV-ETS station (up to $659 \pm 500\%$) suggest the influence of localised seafloor sources, such as
450 cold seeps or shallow gas venting, which are well documented in the Levantine sub-basin (Coleman and Ballard, 2001). Alternatively, nearshore/river filaments or submarine groundwater discharge (SGD), which can be brackish to saline and may not show as a salinity minimum, can significantly raise CH₄, SST, and salinity remain mostly unchanged. In this region, the presence of coastal groundwater systems and SGD is supported by hydrogeochemical/isotopic evidence for the Mersin–
455 Erdemli and Lamas areas (Kuyumcu, 2023). Both scenarios, seafloor sources and SGD, can likely contribute to the episodic enrichment of surface waters in this region, however further research is needed to confirm them.

In contrast, N₂O concentrations showed much lower spatial variability, with station averages ranging from 7.2 ± 0.7 nmol kg⁻¹ (LEV-ETS) to 8.5 ± 0.3 nmol kg⁻¹ (ALB-M'DIQ) (Table 2, Fig. 3). The N₂O
460 distribution showed an inverse relationship with SST, and significant differences (Tukey, $p < 0.05$)



were observed only between the Eastern and Western extremes of the Mediterranean Sea. Notably, N_2OSat levels followed an opposite longitudinal trend to absolute concentrations, with higher values at the Eastern Basin (ranging from $100\pm 4\%$ at BAL-CS to $116\pm 11\%$ in the Levantine stations). Despite the widespread N_2O oversaturation, these values remain relatively low compared to those
465 in other coastal seas (Charpentier et al., 2007; Sommer et al., 2025). This finding suggests that both external inputs and in situ biological production, such as nitrification and denitrification processes in the water column or benthic compartment, are comparatively weak in coastal waters of the studied stations, consistent with the ultra-oligotrophic nature of the Mediterranean Sea.

Nutrient concentrations reflected a predominantly oligotrophic regime, although episodic enrichment
470 was observed near the coast (Table 2). Maximum values of nitrate (up to $7.78 \mu M$ at LEV-BEY) and phosphate (up to $6.23 \mu M$ at LEV-B1) suggest localized continental influence. Specifically, the elevated silicate levels in the Eastern Basin (mean $>2 \mu M$) coupled with high nutrient peaks point towards terrestrial runoff and potential anthropogenic inputs from major coastal urban centers as the primary drivers of coastal nutrient variability. Nutrient stoichiometry indicated a shift from the typical
475 phosphorus-limited regime of the open Mediterranean towards nitrogen-limited conditions in several coastal sites. Specifically, low N:P ratios (<10) in stations such as LEV-B1 and BAL-CA, coupled with high silicate concentrations (up to $5.61 \mu mol \cdot L^{-1}$), suggest a strong influence of terrestrial runoff and urban effluents. This is consistent with the description of the study sites (Section 2.1), where the proximity of anthropogenic activities is identified as a potential driver of local biogeochemical
480 variability. The highest phytoplankton biomass was recorded at LEV-BEY (mean $0.45\pm 0.22 \mu g \cdot L^{-1}$), where a more balanced N:P ratio (≈ 18.7) appears to support enhanced primary production compared to the more nitrogen-limited eastern sites.

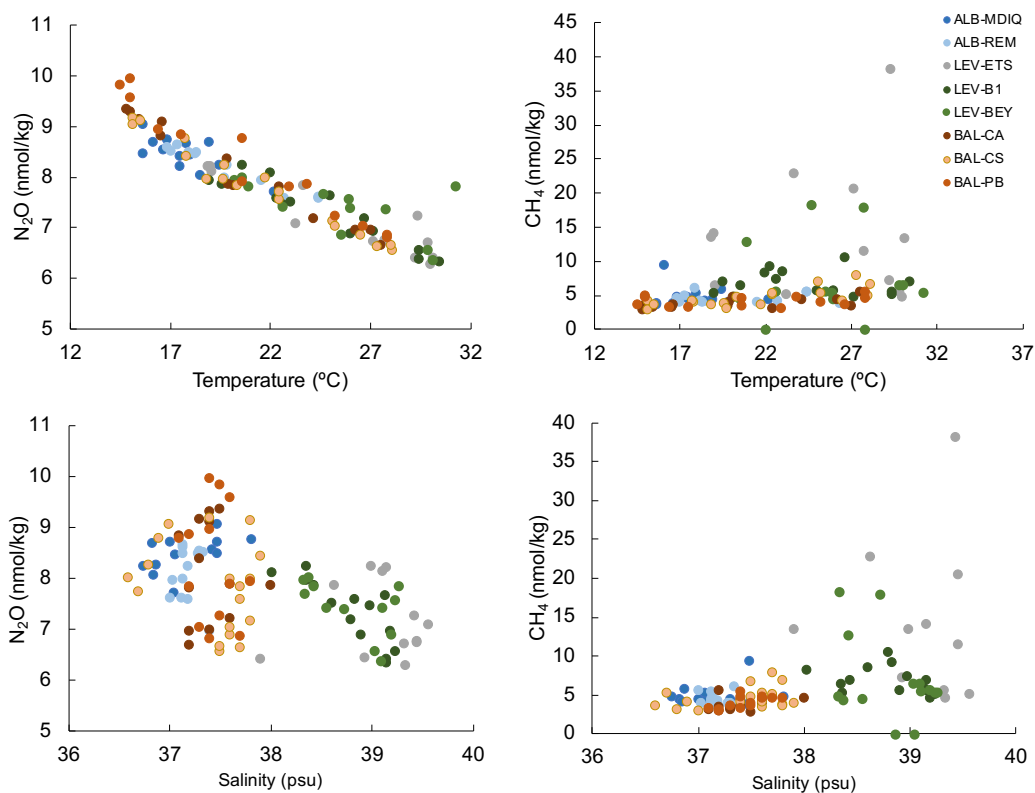


485 **Figure 3.** West to East spatial distribution of box-plot for surface temperature (°C), salinity, concentration of N₂O and CH₄ in nmol kg⁻¹ and saturation percentage of N₂O (N₂OSat) and CH₄ (CH₄Sat).

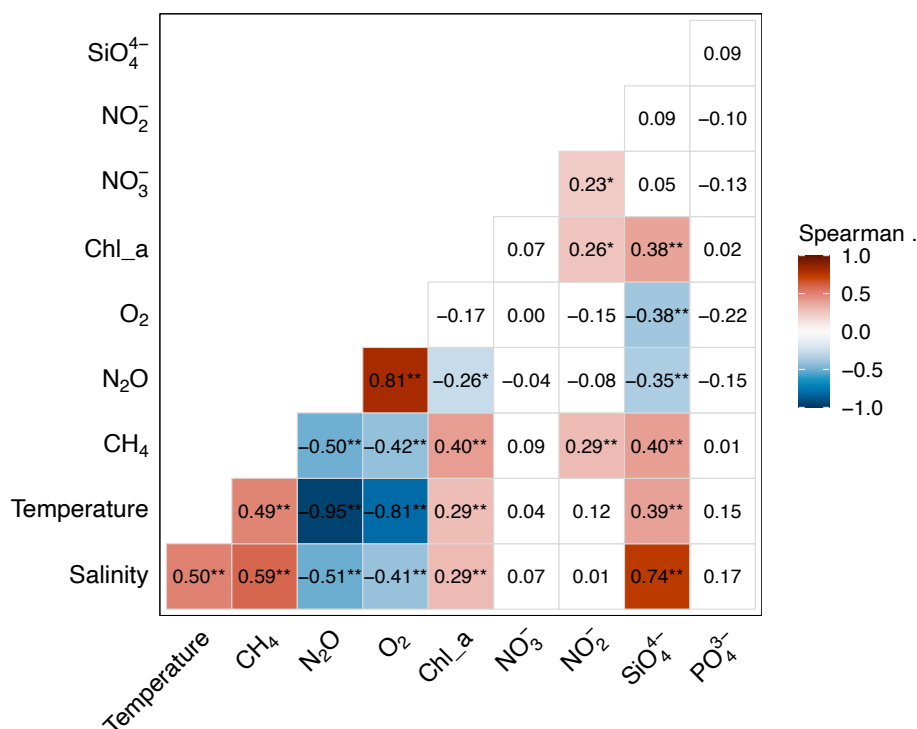


3.3. Correlation of surface N₂O and CH₄ with environmental variables

The N₂O concentrations showed a strong negative correlation with temperature for the entire database collected from all study sites; showing that both the temporal and spatial scales of variability were highly controlled by temperature (Fig. 4). This negative correlation points to a thermodynamic control of the variability through solubility, which increases N₂O in colder water. However, there was a positive correlation between N₂OSat and temperature, with higher values in summer in the Eastern Basin than in winter in the Western Basin, corresponding to an enhancement of N₂O microbial production with increasing temperature. In contrast, CH₄ concentrations showed the opposite behaviour to N₂O, with greater variability and a positive correlation with temperature, indicating mechanisms other than solubility controlling the variability and important sources of CH₄ in the Eastern Basin.



500 **Figure 4.** Scatter plots illustrating the relationship between dissolved N₂O and CH₄ concentrations (nmol kg⁻¹) and key environmental variables: surface water temperature (°C) and salinity. Data from all stations are included, highlighting the overall trends across the Mediterranean Basin



505 **Figure 5.** Spearman's rank correlation matrix showing the interrelationships between N₂O and CH₄
 concentrations and various environmental parameters (temperature, salinity, dissolved oxygen, nutrients,
 chlorophyll a) for the entire dataset, excluding data from LEV-ETS due to missing ancillary variables. Significant
 correlations are indicated with asterisk (**: $p < 0.01$; *: $p < 0.05$).

510

The Spearman correlation matrix accounts for overall variability at both temporal and spatial scales,
 as shown in Fig. 5 for N₂O and CH₄ concentrations. The correlation analysis showed that N₂O was
 strongly correlated with temperature (-0.95 , $p < 0.01$) and significantly negatively correlated with
 salinity (-0.51 , $p < 0.01$), Chl a (-0.26 , $p < 0.05$), and silicate (-0.35). ($p < 0.01$) and was highly
 positively correlated with O₂ ($r = 0.81$, $p < 0.01$). The CH₄ showed an opposite behaviour, with a
 significant negative correlation with oxygen (-0.42 , $p < 0.01$) and positive correlation with salinity (r
 = 0.59 , $p < 0.01$), temperature (0.49 , $p < 0.01$), Chl a (0.4 , $p < 0.01$), and silicate (0.4 , $p < 0.01$).
 Temperature was clearly the main controlling factor, especially for N₂O, and the overall correlation
 with salinity was stronger than when the analysis was performed at every station. This could be due
 to the higher salinity in the Levantine Sea and the zonal distribution pattern of salinity in the basin
 itself. Furthermore, the analysis of the Spearman correlation matrix for each station revealed
 additional local mechanisms acting on the seasonal scale that could be relevant, such as a significant
 positive correlation in O₂ among Western Mediterranean stations (BAL-CA, BAL-CS, BAL-PB, and
 BAL-REM) that was not significant in the eastern Levantine sub-basin. In addition, the strong

520



525 negative correlation between N_2O and temperature was ubiquitous across stations but was only correlated with salinity in LEV-B1 (negative correlation) and ALB-M'DIQ (positive correlation). Finally, Chl *a* was only significant for temporal variability at the LEV-BEY and BAL-CS stations.

Our study is consistent with previous studies in the Eastern (Bange et al., 1996) and Western
530 Mediterranean Sea (de la Paz et al., 2015, Flecha et al., 2023, 2025), where temperature was revealed to be the main controlling factor of surface N_2O and CH_4 variability.

3.4 Air-sea fluxes of N_2O and CH_4

Surface waters were consistently supersaturated with CH_4 relative to the atmosphere at all the
535 coastal Mediterranean stations (Table 2). Consequently, the region acted as a net CH_4 source, with air-sea flux exhibiting high temporal variability (Table 3). Fluxes ranged from 0.97 to 11.41 $\mu\text{mol m}^{-2} \text{d}^{-1}$ in the Balearic sub-basin, 1.74 to 15.4 $\mu\text{mol m}^{-2} \text{d}^{-1}$ in the Alboran sub-basin, and reached a maximum of 35.2 $\mu\text{mol m}^{-2} \text{d}^{-1}$ in the Levantine Sea (Fig. 6, Table 2). While no uniform seasonal trend was observed basin-wide, a notable regional decoupling occurred: maximum CH_4 outgassing
540 in the Balearic sub-basin (July–November 2023) coincided with the lowest flux periods in the Alboran and Levantine sub-basins.

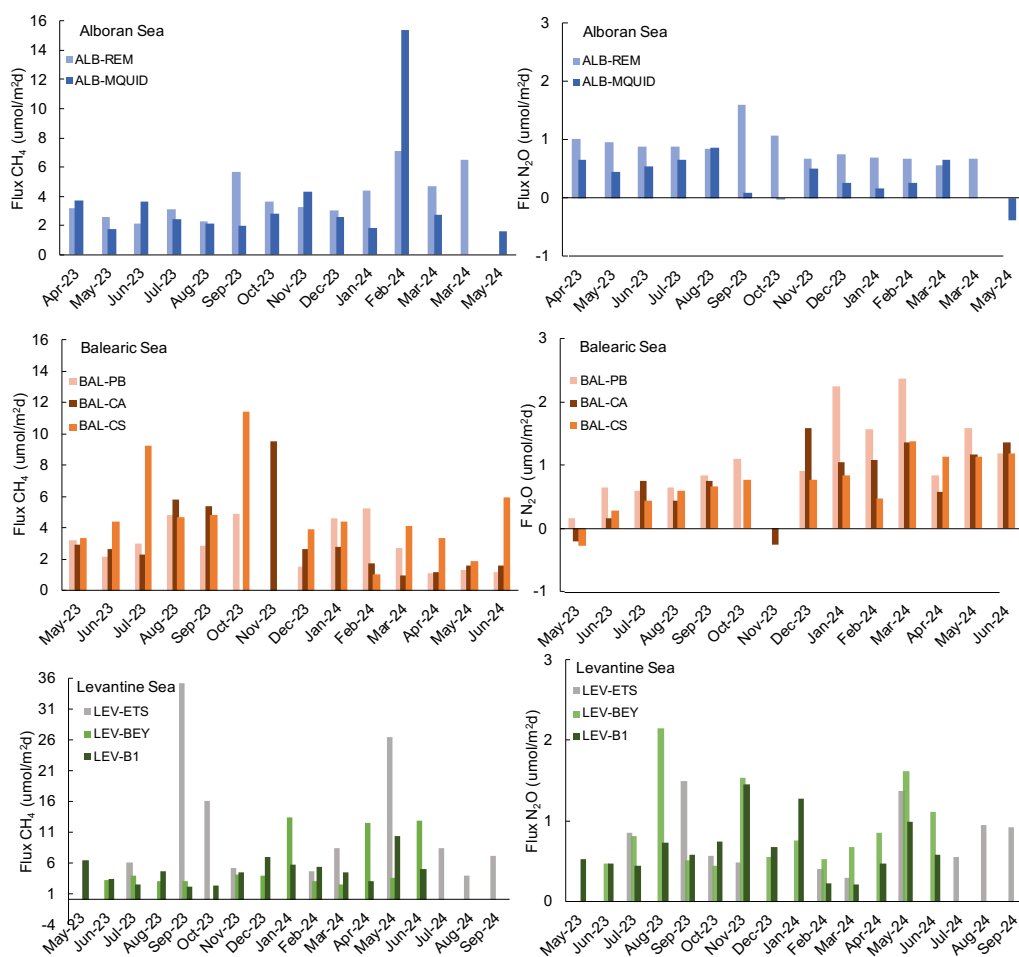
In contrast, N_2O Sat and subsequent air-sea exchange followed a more distinct seasonal trend. Most stations remained moderately supersaturated, acting as a minor N_2O source, with the exception of
545 brief undersaturation events (>98%) in the Balearic sub-basin in May and November 2023. N_2O fluxes peaked in the Balearic sub-basin at 2.37 $\mu\text{mol m}^{-2} \text{d}^{-1}$ (January 2024), driven by a combination of supersaturation and intensified winter wind speeds in the Western Mediterranean. Overall, the N_2O flux variability mirrored seasonal concentration changes but was strongly modulated by wind-driven gas transfer.

550 The annual flux average (Table 3) confirmed that all stations behaved as net annual sources of both CH_4 and N_2O . The highest mean CH_4 fluxes were recorded at the Erdemli site (LEV-ETS: 13.68±9.57 $\mu\text{mol m}^{-2} \text{d}^{-1}$). At this site, the substantial discrepancy between the mean and median (8.39 $\mu\text{mol m}^{-2} \text{d}^{-1}$) highlights a heavily right-skewed distribution caused by episodically high-concentration events unique to the Levantine Sea. Conversely, annual N_2O fluxes were remarkably homogeneous across subbasins, ranging from 0.42±0.26 $\mu\text{mol m}^{-2} \text{d}^{-1}$ (ALB-M'DIQ) to 1.11±0.64 $\mu\text{mol m}^{-2} \text{d}^{-1}$ (BAL-PB), showing a symmetric distribution with closely aligned mean and median values.

The magnitude of the air-sea fluxes calculated in this study is consistent with the sparse literature
560 on the Mediterranean Sea. Our CH_4 fluxes in the Alboran sub-basin (1.74 to 15.4 $\mu\text{mol m}^{-2} \text{d}^{-1}$) aligned with the ranges reported by de la Paz et al. (2015) in the Strait of Gibraltar and the recent



565 observations by Flecha et al. (2023, 2025), who highlighted the coastal Alboran and Balearic seas as persistent sources of CH₄ emissions. The annual mean fluxes of N₂O (0.42 to 1.11 μmol m⁻² d⁻¹) are in excellent agreement with the values reported by Bange et al. (1996) for the Aegean Sea (0.1 to 1.2 μmol m⁻² d⁻¹), confirming that both the Eastern and Western basins act as moderate but steady sources of N₂O to the atmosphere. However, the episodic high-flux events recorded at the LEV-ETS station represent some of the highest CH₄ emission rates documented for the offshore Levantine sub-basin, emphasising the role of localised coastal hotspots in the regional greenhouse gas budget.



570 **Figure 6.** Time-series of air-sea fluxes of N₂O and CH₄ for each station, shown by marine ecoregions.



575 **Table 3.** Range (min-max) of air-sea fluxes for each station, and median and average annual N₂O and CH₄ air-sea flux ($\mu\text{mol m}^{-2} \text{d}^{-1}$) calculated using the expression for gas exchange rate proposed by Wanninkhof (2014).

	Site Station Code	F CH ₄ ($\mu\text{mol m}^{-2} \text{d}^{-1}$)			F N ₂ O ($\mu\text{mol m}^{-2} \text{d}^{-1}$)		
		Range	Median	Mean \pm SD	Range	Median	Mean \pm SD
Balearic Sea	BAL-CA	1-9.6	2.73	3.80 \pm 2.59	-0.25-1.58	0.75	0.67 \pm 0.55
	BAL-CS	1-11.4	4.40	5.46 \pm 3.09	-0.27-1.37	0.71	0.68 \pm 0.42
	BAL-PB	1.1-5.2	3.10	3.36 \pm 1.23	0.16-2.37	0.87	1.11 \pm 0.64
Levantine Sea	LEV-B1	2.1-10.3	4.47	4.57 \pm 2.23	0.21-1.45	0.63	0.69 \pm 0.69
	LEV-BEY	2.5-13.4	3.60	4.99 \pm 3.59	0.47-2.15	0.78	0.95 \pm 0.51
	LEV-ETS	4.5-35.2	8.39	13.68 \pm 9.57	0.3-1.49	0.65	0.79 \pm 0.39
Alboran Sea	ALB-M'DIQ	1.7-15.4	2.67	3.79 \pm 3.59	-0.03-0.86	0.48	0.42 \pm 0.26
	ALB-REM	2.1-7.1	3.26	3.77 \pm 1.41	0.56-1.58	0.86	0.88 \pm 0.26

580 **Table 4.** Annual average N₂O and CH₄ air-sea flux ($\mu\text{mol m}^{-2} \text{d}^{-1}$) for this study and other data published data in the Mediterranean Sea.

Region	Reference	Flux CH ₄ ($\mu\text{mol m}^{-2} \text{d}^{-1}$)	Flux N ₂ O ($\mu\text{mol m}^{-2} \text{d}^{-1}$)
Strait of Gibraltar	de la Paz et al. (2015)	0 - 1.68	0.35 \pm 0.27
Balearic Sea	Flecha et al. (2023/25)	~0.2 - 9.7 (1.4 \pm 1.4)	-0.3-0.6 (0.1 \pm 0.2)
Aegean Sea	Bange et al. (1996)	0.26-14.5 (mean 1.7)	0.1 - 1.7
Alboran Sea	This study	3.8 \pm 3.6	0.9 \pm 3
Balearic Sea	This study	4.2 \pm 1.3	0.8 \pm 0.5
Levantine Sea	This study	7.7 \pm 5.1	0.8 \pm 0.5

4. Data availability

Data described in this paper are accessible at the Zenodo repository <https://doi.org/10.5281/zenodo.19351642> (de la Paz et al.,2026). During the peer-review process, anonymous access is restricted via DOI until publication; however, data are available upon email request to the corresponding author for other interested parties



6. Conclusions

590 This data paper presents the first comprehensive, seasonally-resolved dataset of N₂O and CH₄
concentrations and air-sea fluxes across under-sampled coastal regions of the Mediterranean Sea.
Our results confirm that these coastal waters consistently act as a net source of both N₂O and CH₄
to the atmosphere. We found a strong thermodynamic control on N₂O variability, with higher
concentrations in colder waters and moderate oversaturation throughout the Mediterranean Sea. In
595 contrast, CH₄ dynamics were highly variable, positively correlated with temperature, and marked by
episodic high-flux events, particularly in the Levantine Sea, indicating the influence of localized
geological or anthropogenic sources. Despite challenges in assessing changes in N₂O and CH₄ in
coastal water due to limited measurements, this dataset contributes to the understanding of
greenhouse gas variability in the region. This quality-controlled ROADSTER dataset provides a
600 valuable regional resource that enables accurate trend quantification and change estimation, serving
as an essential baseline for evaluating environmental impacts, refining regional non-CO₂
greenhouse gas budgets, and improving global climate models.

11. Author contribution

605 MdIP conducted the sample analyses, performed the data analyses, and wrote the first draft of
the manuscript. SF, FB, MF, VI, KÖ, and IEH collected samples. SF, MdP and AERH
contributed to the design of the study. FFP contributed to data analysis. IEH designed and led
the study. All authors contributed to discussions on sample design and collection and data
analysis, and reviewed, revised, and approved the final version of the manuscript.

610 12. Competing interests

The contact author has declared that none of the authors has any competing interests

15. Acknowledgements

615 Data has been collected and analysed within the project *COOPB22023 of the i-COOP 2022* call from
the Spanish Research Council (CSIC). Sampling in the Balearic Sea has been enabled through the
Balearic Ocean Acidification Time Series (BOATS) with financial support of PID2021-123723OB-
C22 (CYCLE) funded by MCIN/AEI/10.13039/501100011033 “ERDF A way of making Europe”. The
present research has been carried out in the framework of the activities of the Spanish Government
through the accreditation “Centro de Excelencia María de Maeztu” to IMEDEA (CSIC-UIB)



620 (CEX2021-001198). VI and KO received logistic and historical data support from DEKOSIM (BAP-
08-11-DPT2012K120880) and TÜBİTAK project no 120Y082 and would like to express gratitude
to Kazım Tutsak, Alaeddin Akkaş, Serhat Ertuğrul, Ganiye Ekmekçi for the sampling efforts at
Erdemli stations and to Mr. Ismail Ennaskhi from the Tangier Regional Center and Mr. Ahmed
Chihani from the Nador Regional Center for their help during the samplings in Morocco. Thanks to
625 X.A. Padin for his assistance providing the data-product wind data CCMP. MdlIP acknowledges the
financial support for the contracts financed by the Spanish Ministry of Science under grant PTA2024-
025174-I. SF staff hired under the Generation D initiative, promoted by Red.es, an organization
affiliated with the Ministry for Digital Transformation and the Civil Service, financed by the Recovery,
Transformation, and Resilience Plan through the European Union's Next Generation funds. This
630 work contributes to the CSIC Interdisciplinary Thematic Platform, OCEANS+.

16. References

- 635 Abboud-Abi Saab, M., Fakhri, M., Hassoun, A.E.R., Tilbian, M., Kassab, M.T. and Matar, N., 2012,
November. Effects of continental input on marine environment in the Lebanese coastal waters. In
INOC-CNRS, International Conference on "Land-Sea Interactions in the Coastal Zone", 06-08
November 2012 (pp. 370-382).
- Arias, P., Bellouin, N., Coppola, E., Jones, R., Krinner, G., Marotzke, J., Naik, V., Palmer, M.,
Plattner, G.-K., Rogelj, J., 2021. Climate Change 2021: The Physical Science Basis. Contribution of
640 Working Group I to the Sixth Assessment Report of the Intergovernmental Panel on Climate
Change; Technical Summary. <https://doi.org/10.1017/9781009157896.002>
- Bange, H.W., Rapsomanikis, S., Andreae, M.O., 1996. The Aegean Sea as a source of atmospheric
nitrous oxide and methane. *Marine Chemistry* 53, 1–2, 41–49. doi: 10.1016/0304-4203(96)00011-4
- 645 Bange, H. W., Arévalo-Martínez, D. L., de la Paz, M., Farías, L., Kaiser, J., Kock, A., Law, C. S.,
Rees, A. P., Rehder, G., Tortell, P. D., Upstill-Goddard, R. C., and Wilson, S. T., 2019. A harmonized
nitrous oxide (N₂O) ocean observation network for the 21st century, *Frontiers in Marine Science*, 6,
157, 10.3389/fmars.2019.00157.
- Bendshneider K. and Robinson, R.-J., 1952. A new spectrophotometric method for the determination
of nitrite in sea water. *J. Mar. Res.*, 11 (1952), pp. 87-96
- 650 Bianchi, C. N. and Morri, C.: Marine biodiversity of the Mediterranean Sea: Situation, problems and
prospects for future research, *Mar Pollut Bull*, 40, 367–376, [https://doi.org/10.1016/S0025-326X\(00\)00027-8](https://doi.org/10.1016/S0025-326X(00)00027-8), 2000.
- Coleman, D.F., Ballard, R.D. A highly concentrated region of cold hydrocarbon seeps in the
southeastern Mediterranean Sea. *Geo-Mar Lett* 21, 162–167 (2001).
655 <https://doi.org/10.1007/s003670100079>
- Charpentier, J., Farías, L., & Pizarro, O. (2007). Nitrous oxide distribution and its origin in the central
and eastern South Pacific Ocean. *Biogeosciences*, 4, 729–741. <https://doi.org/10.5194/bg-4-729-2007>.
- 660 Ciais, Philippe, Sabine, C., Bala, G., Bopp, L., Brovkin, V., Canadell, J., Chhabra, A., DeFries, R.,
Galloway, J., Heimann, M., Jones, C., Quéré, C. le, Myneni, R.B., Piao, S., Thornton, P., 2013. The
physical science basis. Contribution of working group I to the fifth assessment report of the
intergovernmental panel on climate change. *Change*, IPCC Climate 465–570.
<https://doi.org/10.1017/CBO9781107415324.015>



- 665 Codispoti, L. A.: Interesting Times for Marine N_2O , *Science* (1979), 327, 1339–1340, <https://doi.org/10.1126/science.1184945>, 2010.
- Damm, E., Thoms, S., Beszczynska-Möller, A., Nöthig, E.M., Kattner, G., 2015. Methane excess production in oxygen-rich polar water and a model of cellular conditions for this paradox. *Polar Sci* 9. <https://doi.org/10.1016/j.polar.2015.05.001>.
- 670 de la Paz, M., Huertas, I.E., Flecha, S., Ríos, A.F., Pérez, F.F., 2015. Nitrous oxide and methane in Atlantic and Mediterranean waters in the Strait of Gibraltar: Air-sea fluxes and inter-basin exchange. *Progress in Oceanography* 138, Part A, 18–31. doi: 10.1016/j.pocean.2015.09.009
- de la Paz, M. and Pérez, F.F., 2026. Greenhouse gas analysis service in natural waters (AQUANITROMET). <http://hdl.handle.net/10261/423686>
- 675 de la Paz, M., Flecha, S., Bouthir, Fatima. Zohra, Fakhri, M., Hassoun, A. E. R., Ibello, V., Özkan, K., Fernandez Perez, F., Adil, C., & Hendriks, I. (2026). Nitrous oxide and methane concentrations and air-sea fluxes in undersampled areas of the Mediterranean basin [Data set]. Zenodo. <https://doi.org/10.5281/zenodo.19351642>
- DOE, 1994. Handbook of Methods for the Analysis of the Various Parameters of the Carbon Dioxide System in Sea Water. Dickson A.G. and Goyet C., pp. 117–124.
- 680 Doney, S. C.: The growing human footprint on coastal and open-ocean biogeochemistry, *Science* (1979), 328, 1512, 2010.
- EEA: State and pressures of the marine and coastal Mediterranean environment, European Environment Agency, 1–44, 1999.
- 685 Escudier, R., Clementi, E., Omar, M., Cipollone, A., Pistoia, J., Aydogdu, A., Drudi, M., Grandi, A., Lyubartsev, V., Lecci, R., Cretí, S., Masina, S., Coppini, G., & Pinardi, N. (2020). Mediterranean Sea Physical Reanalysis (CMEMS MED-Currents) (Version 1) [Data set]. Copernicus Monitoring Environment Marine Service (CMEMS). https://doi.org/10.25423/CMCC/MEDSEA_MULTIYEAR_PHY_006_004_E3R1
- 690 Fach, B. A., Orek, H., Yilmaz, E., Tezcan, D., Salihoglu, I., Salihoglu, B., & Latif, M. A. (2021). Water mass variability and levantine intermediate water formation in the Eastern Mediterranean between 2015 and 2017. *Journal of Geophysical Research: Oceans*, 126(2), e2020JC016472.
- Flecha, S., Rueda, D., de la Paz, M., Pérez, F. F., Alou-Font, E., Tintoré, J., and Hendriks, I. E.: Spatial and temporal variation of methane emissions in the coastal Balearic Sea, *Western Mediterranean, Science of the Total Environment*, 865, <https://doi.org/10.1016/j.scitotenv.2022.161249>, 2023.
- Flecha, S., de la Paz, M., Pérez, F. F., Marbà, N., Morell, C., Alou-Font, E., Tintoré, J., and Hendriks, I. E. Drivers of the spatiotemporal distribution of dissolved nitrous oxide and air-sea exchange in a coastal Mediterranean area, *Ocean Science*, 21, 1515–1532, 2025. <https://doi.org/10.5194/os-21-1515-2025>.
- 700 Freing, A., Wallace, D. W. R., and Bange, H. W.: Global oceanic production of nitrous oxide, *Philosophical Transactions of the Royal Society B: Biological Sciences*, 367, 1245–1255, <https://doi.org/10.1098/rstb.2011.0360>, 2012.
- Grasshoff, F.K. , 1961. Zur bestimmung von nitrat in meer-und trink wasser. *Kieler Muresforsch*, 20 (1961), pp. 5-10
- 705 Hansen, H.P., 1999. Determination of oxygen. *Methods of seawater analysis*. In: Grasshoff, M., Kremling, K., Ehrhardt, M. (Eds.), Verlag Chemie, Weinheim, pp. 75–89.
- Hassoun A.E.R., Bantelman A., Melaku Canu D., Comeau S., Galdies C., Gattuso J.-P., Giani M., Grelaud M., Hendriks I., Ibello V., Idrissi M., Krasakopoulou E., Shaltout N., Solidoro C., Swarzenski P., and Ziveri P., 2022. Ocean Acidification Research in the Mediterranean Sea: Status, Trends and



- 710 Next Steps. *Front. Mar. Sci. Sec. Marine Biogeochemistry*, [Frontiers | Ocean acidification research in the Mediterranean Sea: Status, trends and next steps \(frontiersin.org\)](#).
Hassoun AER, Tanhua T, Heslop E, Lips I, Álvarez M, Petihakis G, García-Ibáñez MI, Velaoras D, Giani M, Bange HW, Lønborg C and Karstensen J (2024) A first scoring approach for evaluating the European Ocean Observing Community. *Front. Mar. Sci.* 11:1466820. doi: 10.3389/fmars.2024.1466820
- 715 Hassoun, A.E.R., R. Hernández-Moresino, E.S. Barbieri, J.C. Carbajal, A. Crespi-Abril, A. De Cian, L. Epherra, M. Fakhri, A. Ghanem, H. Jaber, M.-T. Kassab, A. Martelli, A. Ouba, F. Paparazzo, J.P. Pisoni, E. Tarek, and J.G. Vázquez. 2021. Coastal monitoring in the context of climate change: Time-series efforts in Lebanon and Argentina. Pp. 12–13 in *Frontiers in Ocean Observing: Documenting Ecosystems, Understanding Environmental Changes, Forecasting Hazards*. E.S. Kappel, S.K. Juniper, S. Seeyave, E. Smith, and M. Visbeck, eds, *A Supplement to Oceanography* 34(4), <https://doi.org/10.5670/oceanog.2021.supplement.02-05>.
- 720 Jatiault, R., Autry Aiken, C. & Klingelhoefer, F. Earthquakes can drive hydrocarbon seepage along the Cyprus Arc. *Commun Earth Environ* 6, 774 (2025). <https://doi.org/10.1038/s43247-025-02556-y>
- 725 Lorenzen, C.-J., 1967. Determination of chlorophyll and pheophytin: spectrophotometric equations. *Limnol. Oceanogr.*, 12 (1967), pp. 343-346
Kuyumcu, B. (2023). Estimating submarine groundwater discharge in the Cilician Basin by radioactive isotope tracers and hydrodynamic modeling (Master's thesis, Middle East Technical University). (METU Open Access handle: 11511/104884).
- 730 Mears, C.; Lee, T.; Ricciardulli, L.; Wang, X.; Wentz, F., 2022: RSS Cross-Calibrated Multi-Platform (CCMP) 6-hourly ocean vector wind analysis on 0.25 deg grid, Version 3.0, Remote Sensing Systems, Santa Rosa, CA. Available at www.remss.com <https://doi.org/10.56236/RSS-uv6h30>
- Merey, Ş., Longinos, S. N. 2019. The gas hydrate potential of the Eastern Mediterranean basin. *Bulletin of the Mineral Research and Exploration*. 160, 117-134.
735 <https://doi.org/10.19111/bulletinofmre.502275>
- MedECC (2020). *Climate and Environmental Change in the Mediterranean Basin – Current Situation and Risks for the Future. First Mediterranean Assessment Report* [Cramer, W., Guiot, J., Marini, K. (eds.)] Union for the Mediterranean, Plan Bleu, UNEP/MAP, Marseille, France, 632pp, ISBN 978-2-9577416-0-1, doi: 10.5281/zenodo.4768833
- 740 Mouillot, D., Albouy, C., Guilhaumon, F., Ben Rais Lasram, F., Coll, M., Devictor, V., Meynard, C. N., Pauly, D., Tomasini, J. A., Troussellier, M., Velez, L., Watson, R., Douzery, E. J. P., and Mouquet, N.: Protected and threatened components of fish biodiversity in the Mediterranean sea, *Current Biology*, 21, 1044–1050, <https://doi.org/10.1016/j.cub.2011.05.005>, 2011.
- Murphy J., and Riley, J.P., 1962. A modified single solution method for the determination of phosphate in natural waters. *Anal. Chim. Acta*, 27 (1962), pp. 31-36
- 745 Ouba, A., Abboud-Abi Saab, M. and Stemmann, L., 2016. Temporal Variability of Zooplankton (2000-2013) in the Levantine Sea: Significant Changes Associated to the 2005-2010 EMT-like Event?. *PLoS One*, 11(7), p.e0158484. <https://doi.org/10.1371/journal.pone.0158484>
- Reeburgh, W.S., 2007. Oceanic methane biogeochemistry. *Chem Rev*.
750 <https://doi.org/10.1021/cr050362v>
- Rees, A.P., Bange, H.W., Arévalo-Martínez, D.L., Artioli, Y., Ashby, D.M., Brown, I., Campen, H.I., Clark, D.R., Kitidis, V., Lessin, G. and Tarran, G.A., 2022. Nitrous oxide and methane in a changing Arctic Ocean. *Ambio*, 51, pp.398-410. <https://link.springer.com/article/10.1007/s13280-021-01633-8>
- 755 Resplandy, L., Hogikyan, A., Müller, J.D., Najjar, R.G., Bange, H.W., Bianchi, D., Weber, T., Cai, W.-J., Doney, S.C., Fennel, K., Gehlen, M., Hauck, J., Lacroix, F., Landschützer, P., Le Quééré, C., Roobaert, A., Schwinger, J., Berthet, S., Bopp, L., Chau, T.T.T., Dai, M., Gruber, N., Ilyina, T., Kock, A., Manizza, M., Lachkar, Z., Laruelle, G.G., Liao, E., Lima, I.D., Nissen, C., Rödenbeck, C.,



- 760 S  ferian, R., Toyama, K., Tsujino, H., Regnier, P., 2024. A Synthesis of Global Coastal Ocean Greenhouse Gas Fluxes. *Global Biogeochemical Cycles* 38, 1, e2023GB007803. doi: 10.1029/2023GB007803
- Rosentreter, J.A., Laruelle, G.G., Bange, H.W. *et al.* Coastal vegetation and estuaries are collectively a greenhouse gas sink. *Nat. Clim. Chang.* **13**, 579–587 (2023). <https://doi.org/10.1038/s41558-023-01682-9>
- 765 Saunois, M., Stavert, A.R., Poulter, B., Bousquet, P., Canadell, J.G., Jackson, R.B., Raymond, P.A., Dlugokencky, E.J., Houweling, S., 2020. The Global Methane Budget 2000 – 2017 1561–1623. <https://doi.org/10.5194/essd-8-697-2016>
- Sommer, M., Bange, H. W., Eisnecker, P., Schulz, G., Stoltenberg, I., & Ar  valo-Mart  nez, D. L. (2025). N₂O emissions from the eastern tropical Indian Ocean. *Geophysical Research Letters*, 52, e2025GL117627. <https://doi.org/10.1029/2025GL117627>
- 770 Strickland J.D.H. and Parsons, T.R., 1968. A practical handbook of seawater analysis. *Bull. Fish. Res. Board Can.*, 167 (1968), p. 311
- Tanhua T., Pouliquen S., Hausman J., O'brien K., Bricher P., De Bruin T., et al. (2019). Ocean FAIR data services. *Front. Mar. Sci.* 6. doi: 10.3389/fmars.2019.00440/full
- 775 Tintor  , J. Gomis D., Alonso S., Parrilla G. 1991. Mesoscale Dynamics and Vertical Motion in the Albor  n Sea Vi  dez   ., Jean-Michel Pinot, R. Haney 1998. On the upper layer circulation in the Alboran Sea
- Wanninkhof, R., 2014. Relationship between wind speed and gas exchange over the ocean revisited: Gas exchange and wind speed over the ocean. *Limnol. Oceanogr. Methods* 12, 6, 351–362. doi: 10.4319/lom.2014.12.351
- 780 Weber, T., Wiseman, N.A., Kock, A., 2019. Global ocean methane emissions dominated by shallow coastal waters. *Nat Commun* 10, 1–10. <https://doi.org/10.1038/s41467-019-12541-7>
- Wentz, F. J., D. K. Smith, R. Hoffman, and R. Atlas, 2015: Cross-Calibrated Multi-Platform (CCMP) Version-2.0 Ocean Surface Wind Vectors. Remote Sensing Systems, Santa Rosa, CA. <https://www.remss.com/measurements/ccmp/>
- 785 Wilson, S.T., Bange, H.W., Ar  valo-Mart  nez, D.L., Barnes, J., Borges, A.V., Brown, I., Bullister, J.L., Burgos, M., Capelle, D.W., Casso, M., de la Paz, M., Farias, L., Fenwick, L., Ferr  n, S., Garcia, G., Glockzin, M., Karl, D.M., Kock, A., Laperriere, S., Law, C.S., Manning, C.C., Marriner, A., Myllykangas, J.-P., Pohlman, J.W., Rees, A.P., Santoro, A.E., Tortell, P.D., Upstill-Goddard, R.C., Wisegarver, D.P., Zhang, G.-L., Rehder, G., 2018. An intercomparison of oceanic methane and nitrous oxide measurements. *Biogeosciences* 15, 19, 5891–5907. doi: <https://doi.org/10.5194/bg-15-5891-2018>
- 790